SCIENCE CHINA
Technological Sciences

doi: 10.1007/s11431-013-5358-3

Theoretical study of piezotronic heterojunction

FENG XiaoLong[1], ZHANG Yan[1,2*] & WANG ZhongLin[1,3*]

[1] *Beijing Institute of Nanoenergy and Nanosystems, Chinese Academy of Sciences, Beijing 100083, China;*
[2] *Institute of Theoretical Physics, Lanzhou University, Lanzhou 730000, China;*
[3] *School of Material Science and Engineering, Georgia Institute of Technology, Atlanta, Georgia 30332-0245, USA*

Received August 17, 2013; accepted September 9, 2013

Due to the coupling of piezoelectric and semiconducting dual properties, much attention has been focused on the piezoelectric semiconductor materials, such as ZnO, ZnS, CdS and GaN. With the usage of these piezoelectric semiconductor materials, novel nanodevices have been demonstrated, from which a new field called piezotronics was formulated. The core of piezotronics is to study the mechanism of the piezoelectric effect on tuning the charge transport behavior across various junctions or interfaces, with potential applications in sensors, microelectromechanical systems, and force/pressure triggered electric devices. Here following the theoretical frame work of piezotronic effect, analytical solutions of piezoelectric heterojunction are presented to investigate the electrical transport behavior at a p-n junction. Numerical simulation is given for guiding future experimental measurements.

Piezoelectric Heterojunction, piezoelectric semiconductor, piezotronics

Citation: Feng X L, Zhang Y, Wang Z L. Theoretical study of piezotronic heterojunction. Sci China Tech Sci, 2013, doi: 10.1007/s11431-013-5358-3

1 Introduction

In recent years, numerous researches have been carried out to investigate the piezoelectric semiconductor materials in the wurtzite family, including zinc oxide, cadmium sulfide, zinc sulfide and gallium nitride [1–6]. Utilizing the coupled piezoelectric and semiconducting property, a variety of novel nanowire-based applications have been demonstrated, such as nanogenerators [7, 8], piezoelectric sensors [9], piezoelectric diodes [10], piezoelectric field-effect transistors [11] and piezo-phototronic devices [12]. In addition, a new field based on the coupling of piezoelectric and semiconducting dual properties was created to investigate the effect of the piezoelectric charges on the electrical transport characteristics to fabricate innovative electromechanical devices, which is named as piezotronics [13–15].

Taking ZnO nanowire as an example, piezoelectric charges will be created at the two ends of the nanowire under a tensile or compress strain. These polarization charges form a piezopotential inside the nanowire, which can tune or control the electrical transport property of the nanowire by changing the local contact of the nanowire with the electrodes from Ohimc contact to Schottky contact and vice versa [16].

Zinc Oxide(ZnO), as a typical material in wurtzite structure family, has attracted great attentions due to the excellent properties, such as the wide direct bang gap of about 3.37 eV and large free-exciton binding energy of 60 meV at room temperature. Furthermore, splendid one-dimensional nanostructures of ZnO have been fabricated [17–20]. Therefore, ZnO is taken as the preferred material to consider piezotronics. To demonstrate the fundamental theory of piezotronics, piezotronic models have been proposed, such as piezoelectric p-n junction and piezoelectric metal-semi-

*Corresponding author (email: zlwang@gatech.edu; yzhang@binn.cas.cn)

© Science China Press and Springer-Verlag Berlin Heidelberg 2013

conductor contact [21, 22]. In these theoretical works the effect of piezoelectric charges on the DC characteristics has been discussed. Numerical simulations also have been given to provide predictions of the carrier transport behavior.

Herein, we extend the analysis for piezoelectric homojunctions to piezoelectric heterojuncitons. We first give the theoretical framework for the piezotronic effect, followed by analytical solutions for p-n GaN-ZnO piezoelectric heterojunction in simplified conditions. Using COMSOL software package, the numerical simulation of the piezoelectric heterojunction is also given to predict the piezotronic device performance. Further experiments about the piezotronic devices can be carried out under the guidance of these theoretical works.

2 Theoretical Framework for Piezotronic Effect

In order to study the piezotronic devices utilizing the coupled semiconducting and piezoelectric properties of wurtzite nanowires, such as ZnO and GaN, theories about piezoelectricity and semiconductor are both required. A coupled set of constitutive equations is employed to describe the basic effects. As to the model of piezoelectric heterojunction, electrostatics equations, current density equations and continuity equations are required to describe the electrical transport properties of the semiconductors [23–26], and piezoelectric equations are also demanded to describe the piezoelectric behavior [27]. For piezotronic and piezo-phototronic devices, heterojunction is a kind of typical device structure. Due to heterojunctions can be formed between two dissimilar lattice-matched semiconductors by epitaxial growing on top of one semiconductor, there are virtually no traps at interface. Therefore, heterojunctions have been widely used in photodetector, solar cell and LED applications. The piezo-charges in heterojunction provide another degree of freedom to dynamically tune/control the carrier generation, transport and recombination processes at the vicinity of a heterojunction. Under straining, the created piezo-charges at the interface of heterjunction change the built-in potential and electric filed. Therefore, the piezo-charges will turn/control the charge transport across the heterojunction, which is similar as piezotronic p-n junction, as described by following equations.

The Poisson equation is to relate the charge distribution with the electric potential distribution as shown in

$$\nabla^2\psi_i = -\frac{\rho(\boldsymbol{r})}{\varepsilon}, \tag{1}$$

where ψ_i is the electric potential distribution, $\rho(\boldsymbol{r})$ is the charge distribution and ε is the dielectric constant of the material.

The current densities for electrons and holes governed by drift and diffusion are

$$\begin{cases} \boldsymbol{J}_{\mathrm{n}} = q\mu_{\mathrm{n}} n\boldsymbol{E} + qD_{\mathrm{n}}\nabla n, \\ \boldsymbol{J}_{\mathrm{p}} = q\mu_{\mathrm{p}} p\boldsymbol{E} - qD_{\mathrm{p}}\nabla p, \\ \boldsymbol{J}_{\mathrm{cond}} = \boldsymbol{J}_{\mathrm{n}} + \boldsymbol{J}_{\mathrm{p}}, \end{cases} \tag{2}$$

where $\boldsymbol{J}_{\mathrm{n(p)}}$ is the electron(hole) current densities, $\mu_{\mathrm{n(p)}}$ is the electron(hole) mobility, n(p) is the concentration of electrons(holes), $D_{\mathrm{n(p)}}$ is the electron(hole) diffusion coefficient, $\boldsymbol{E}$ is the applied electric field and $\boldsymbol{J}_{\mathrm{cond}}$ is the total current density.

The continuity equations for electrons and holes are given by

$$\begin{cases} \dfrac{\partial n}{\partial t} = G_{\mathrm{n}} - U_{\mathrm{n}} + \dfrac{1}{q}\nabla\cdot\boldsymbol{J}_{\mathrm{n}}, \\ \dfrac{\partial p}{\partial t} = G_{\mathrm{p}} - U_{\mathrm{p}} - \dfrac{1}{q}\nabla\cdot\boldsymbol{J}_{\mathrm{p}}, \end{cases} \tag{3}$$

where $G_{\mathrm{n(p)}}$ is the electron (hole) generation rate, $U_{\mathrm{n(p)}}$ is the recombination rate of electrons(holes).

The direct piezoelectric effect results from the spontaneous and piezoelectric polarization caused by the applied strain. The direct effect can be formulated as a linear relation via the material property known as the piezoelectric constant $(\boldsymbol{e})_{ijk}$ which is a third rank tensor as shown in [28]

$$(\boldsymbol{P})_i = (\boldsymbol{e})_{ijk}(\boldsymbol{S})_{jk}. \tag{4}$$

Equations of piezoelectricity are presented as the coupling of electrical behavior and mechanical behavior. The stress-charge form of constitutive relations [27] is written as

$$\begin{cases} \boldsymbol{T} = \boldsymbol{c}_{\mathrm{E}}\boldsymbol{S} - \boldsymbol{e}^{\mathrm{T}}\boldsymbol{E}, \\ \boldsymbol{D} = \boldsymbol{e}\boldsymbol{S} + \varepsilon_{\mathrm{S}}\boldsymbol{E}, \end{cases} \tag{5}$$

where $\boldsymbol{T}$ is the stress tensor, c_{E} is the elastic tensor, ε_{S} is the dielectric tensor, $\boldsymbol{D}$ is the electric displacement and $\boldsymbol{E}$ is the electric field vector.

3 Analytical solution for 1D simplified piezoelectric heterojunction

It is known that p-n junctions is the basis of the modern electronic devices and p-n junction theory is the foundation of the physics of semiconductor devices [24]. Based on analytical solution for piezoelectric p-n junctions [21], solution for piezoelectric heterojunction is investigated. As to heterojunctions, there are dozens of proposed models [29, 30]. Taking Anderson's model as an example, it is on the basis of Shockley's homojunction diffusion theory. For simplicity, we describe the piezoelectric heterojunction using Anderson's theory. The current-voltage characteristics of the piezoelectric heterojunction is analyzed on basis of drift-diffusion model. Interface states and other anomalies are neglected in our proposed model. With slight modifica-

tion, it can be available for non-ideal cases.

Similar to our previous work of the piezoelectric homojunction [21], the electrical contacts of the boundaries are considered as ideal ohmic contacts, which means the carrier concentrations and electrical potential will have Dirichlet boundary conditions. For piezoelectric heterojunctions, the following assumptions are also applied to investigate the current-voltage characteristics: 1)The abrupt depletion layer approximation applies; 2) Both sides of the heterojunction are non-degenerate so that the carrier densities are related to the quasi-Fermi levels through Boltzmann relation; 3) Compared to the majority carrier densities, the injected minority carrier densities are much lower; 4) Inside the depletion layer there is no generation-recombination current, and the electron and hole currents are constant across the depletion layer [24].

We first consider the thermal equilibrium condition without applied voltage and current flow. The charge distribution in the depletion region is assumed to be a box profile, from which the electric field and potential distribution can be obtained. Also the built-in potential and energy band can be figured out. From the Poisson equation we obtain

$$\frac{\mathrm{d}^2\psi_i}{\mathrm{d}x^2} = -\frac{\mathrm{d}E}{\mathrm{d}x} = -\frac{\rho(x)}{\varepsilon}, \tag{6}$$

where

$$\rho(x) = q[N_\mathrm{D}(x) - n(x) - N_\mathrm{A}(x) + p(x) + \rho_\mathrm{piezo}(x)] \tag{7}$$

is the charge density as shown in Figure 1(a), $N_\mathrm{D}(x)$ is the donor concentration, $N_\mathrm{A}(x)$ is the acceptor concentration, $\rho_\mathrm{piezo}(x)$ is the density of piezoelectric charges. Then we can calculate the electric field by integrating the Poisson equation. The results are displayed in Figure 1(b).

$$E(x) = -\frac{qN_\mathrm{A}(x+W_\mathrm{Dp})}{\varepsilon_\mathrm{p}}, \quad \text{for} \quad -W_\mathrm{Dp} \leqslant x \leqslant 0, \tag{8a}$$

$$E(x) = -\frac{qN_\mathrm{D}(W_\mathrm{Dn}-x) + \rho_\mathrm{piezo}(W_\mathrm{piezo}-x)}{\varepsilon_\mathrm{n}}, \quad \text{for} \quad 0 \leqslant x \leqslant W_\mathrm{piezo}, \tag{8b}$$

$$E(x) = -\frac{qN_\mathrm{D}(W_\mathrm{Dn}-x)}{\varepsilon_\mathrm{n}}, \quad \text{for} \quad W_\mathrm{piezo} \leqslant x \leqslant W_\mathrm{Dn}. \tag{8c}$$

According to the electric field, the electric potential can be calculated by integrating the above equations once again by setting $\psi(-W_\mathrm{Dp})$=0 as shown in Figure 1(c).

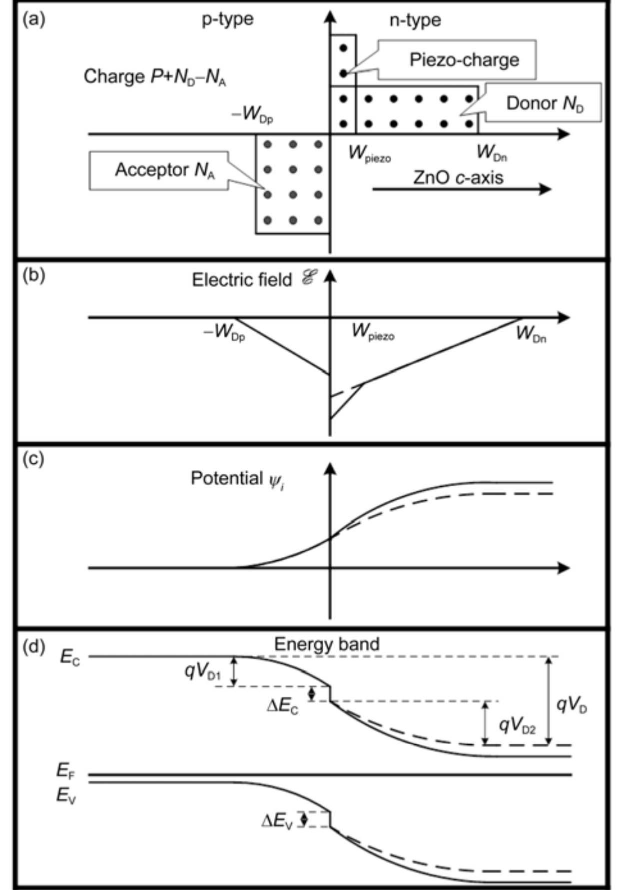

Figure 1 Piezoelectric p-n heterojunction with the presence of piezoelectric charges without applied voltage. (a) Space-charge distribution with the presence of piezoelectric charge without applied voltage; (b) electric-field distribution; (c) potential distribution; (d) energy-band diagram. The dashed lines illustrate the case without the piezoelectric charges while the solid lines illustrate the case in the presence of the piezoelectric charges.

$$\psi(x) = \frac{qN_\mathrm{A}(x+W_\mathrm{Dp})^2}{\varepsilon_\mathrm{p}}, \quad \text{for} \quad -W_\mathrm{Dp} \leqslant x \leqslant 0, \tag{9a}$$

$$\psi(x) = \psi(0) + \left[qN_\mathrm{D}\left(W_\mathrm{Dn}-\frac{x}{2}\right)x + \rho_\mathrm{piezo}\left(W_\mathrm{piezo}-\frac{x}{2}\right)x\right]\Big/\varepsilon_n, \quad \text{for} \quad 0 \leqslant x \leqslant W_\mathrm{piezo}, \tag{9b}$$

$$\psi(x) = \psi(W_\mathrm{piezo}) + qN_\mathrm{D}\left(W_\mathrm{Dn}-\frac{x}{2}\right)x\Big/\varepsilon_\mathrm{n}, \quad \text{for} \quad W_\mathrm{piezo} \leqslant x \leqslant W_\mathrm{Dn}. \tag{9c}$$

Therefore, the built-in potential $\psi_{\mathrm{b}i}$ is given by

$$\psi_{\mathrm{b}i} = \frac{qN_\mathrm{A}W_\mathrm{Dp}^2}{2\varepsilon_\mathrm{p}} + \frac{qN_\mathrm{D}W_\mathrm{Dn}^2}{2\varepsilon_\mathrm{n}} + \frac{q\rho_\mathrm{piezo}W_\mathrm{piezo}^2}{2\varepsilon_\mathrm{n}}, \tag{10}$$

where $\varepsilon_{\mathrm{n(p)}}$ is the permittivity of the n(p)-type semiconductor, $N_{\mathrm{A(D)}}$ is the acceptor(donor) concentration, $\rho_\mathrm{piezo}(x)$

is the density of polarization charges, W_{piezo} is the width of the piezoelectric charges distribution region and $W_{\mathrm{Dp(Dn)}}$ is the depletion layer width in the p(n)-side. Eq. (10) suggest that piezoelectric charges can modify the built-in potential, which relates to the Fermi level. As the piezoelectric charges is assume to be distributed at a region much shorter than the depletion layer ($W_{\mathrm{Dn}} \gg W_{\mathrm{piezo}}$), the effect of piezoelectric charges on ZnO energy band can be considered as a perturbation.

Similar to a regular p-n junction, the electron and hole diffusion currents throughout the piezoelectric heterojunction can be obtained by solving eq. (2) [24]. The results are

$$J_{\mathrm{n}} = q\frac{D_{\mathrm{n1}}}{L_{\mathrm{n1}}}n_{10}\left[\exp\left(\frac{qV}{kT}\right)-1\right], \tag{11a}$$

$$J_{\mathrm{p}} = q\frac{D_{\mathrm{p2}}}{L_{\mathrm{p2}}}p_{20}\left[\exp\left(\frac{qV}{kT}\right)-1\right], \tag{11b}$$

where $D_{\mathrm{n1(p2)}}$ is the electron(hole) diffusion coefficient in p(n)-type semiconductor, $L_{\mathrm{n1(p2)}}$ is the electron(hole) diffusion length in p(n)-type semiconductor, n10(p20) is the equilibrium electron (hole) density in p(n)-type semiconductor, and V is the applied voltage. It should be noted that the band offsets ΔE_{C} and ΔE_{V} are not in these equations, and each diffusion current component depends on the properties of the receiving side only, as in the case of a homojunction.

If E_{F0} is defined as the Fermi level of ZnO in the absence of piezopotential, the Fermi level of ZnO E_{F2} in the presence of piezoelectric charges is given by

$$E_{\mathrm{F2}} = E_{\mathrm{F0}} - q^2\rho_{\mathrm{piezo}}W_{\mathrm{piezo}}^2/(2\varepsilon_{\mathrm{n}}). \tag{12}$$

For

$$p_{20} = n_{i2}\exp\left(\left(E_{i2}-E_{\mathrm{F2}}\right)/kT\right), \tag{13}$$

where n_{i2} is the intrinsic electron density of ZnO, E_{i2} is the intrinsic Fermi level of ZnO, the hole diffusion current can be rewritten as

$$\begin{aligned} J_{\mathrm{p}} &= q\frac{D_{\mathrm{p2}}}{L_{\mathrm{p2}}}n_{i2}\exp\left(\frac{E_{i2}-E_{\mathrm{F2}}}{kT}\right)\left[\exp\left(\frac{qV}{kT}\right)-1\right] \\ &= q\frac{D_{\mathrm{p2}}}{L_{\mathrm{p2}}}n_{i2}\exp\left(\frac{E_{i2}-E_{\mathrm{F0}}}{kT}\right)\exp\left(\frac{q^2\rho_{\mathrm{piezo}}W_{\mathrm{piezo}}^2}{2\varepsilon_n}\right) \\ &\quad\times\left[\exp\left(\frac{qV}{kT}\right)-1\right]. \end{aligned} \tag{14}$$

Thus, the total current density is

$$\begin{aligned} J &= q\left[\frac{D_{\mathrm{n1}}}{L_{\mathrm{n1}}}n_{10} + \frac{D_{\mathrm{p2}}}{L_{\mathrm{p2}}}n_{i2}\exp\left(\frac{E_{i2}-E_{\mathrm{F0}}}{kT}\right)\right. \\ &\quad\left.\times\exp\left(\frac{q^2\rho_{\mathrm{piezo}}W_{\mathrm{piezo}}^2}{2\varepsilon_{\mathrm{n}}}\right)\right]\left[\exp\left(\frac{qV}{kT}\right)-1\right]. \end{aligned} \tag{15}$$

The result suggests that hole diffusion current density is an exponential function of the piezo-charges, which means that the total current can be tuned by controlling the sign and magnitude of the strain. This is the theoretical mechanism of the piezoelectric heterojunction.

4 Numerical simulation of piezoelectric heterojunction

The analytical solutions present the basic physics of piezoelectric heterojunction. Generally, equations also can be solved numerically. With the help of the COMSOL software package, we demonstrate an approach to simulating the piezoelectric heterojunction taking the recombination of carriers into account. In our model, GaN and ZnO are selected to be the p-type and n-type material, respectively. For GaN and ZnO have a low lattice mismatch of about 1.8%, it is applicable to neglect the interface states.

We study the DC characteristics of the piezoelectric heterojunction first. The applied strain is thought to be uniform at the ends of the n-type ZnO nanowire and the distribution of piezo-charges derives from eqs. (4) and (5). The electrical contacts of the device with the electrodes are supposed to be ideal Ohmic contacts and Dirichlet boundary conditions are applied.

To match practical experimental conditions, the Gaussian profile is adopted for the numerical simulation to describe the dopant concentration distribution. The dopant concentration function N is

$$\begin{aligned} N = N_{\mathrm{Dn}} + N_{\mathrm{Dn\,max}}\exp\left[-\left(\frac{z-l}{ch}\right)^2\right] \\ - N_{\mathrm{Ap\,max}}\exp\left[-\left(\frac{z}{ch}\right)^2\right], \end{aligned} \tag{16}$$

where N_{Dn} is the n-type background doping concentration due to the intrinsic defects, $N_{\mathrm{Dn\,max}}$ is the maximum donor doping concentration, $N_{\mathrm{Ap\,max}}$ is the maximum acceptor doping concentration, l is the length of the device, and ch is the doping fall-off constant. N is assigned to be negative in p-type region and positive in n-type region.

The electron and hole generation rates are $G_{\mathrm{p}}= G_{\mathrm{n}}=0$ for no external optical excitations exist in our model. The Shockley-Read-Hall recombination taken as an example of carrier recombination mechanisms is given by

$$U_{\mathrm{p}} = U_{\mathrm{n}} = U_{\mathrm{SRH}} = \frac{np-n_i^2}{\tau_{\mathrm{p}}(n+n_i)+\tau_{\mathrm{n}}(p+n_i)}, \tag{17}$$

where $\tau_{\mathrm{p(n)}}$ is the hole(electron) life time. Therefore, the basic equations can be rewritten as

$$\begin{cases} \nabla^2 \psi_i = -\dfrac{q}{\varepsilon}(p - n + N + \rho_{\text{piezo}}), \\ -\nabla \cdot \boldsymbol{J}_{\text{n}} = -qU_{\text{SRH}}, \\ -\nabla \cdot \boldsymbol{J}_{\text{p}} = qU_{\text{SRH}}. \end{cases} \tag{18}$$

For Dirichlet boundary conditions are applied at the contact electrodes of the device, the electrical potential and the carrier concentration can be given by their thermal equilibrium values as:

$$\psi = \frac{kT}{q}\ln\left(\frac{\frac{N}{2}+\sqrt{\left(\frac{N}{2}\right)^2+n_i^2}}{n_i}\right)-\frac{\chi}{q}+V, \tag{19a}$$

$$n = \frac{N}{2}+\sqrt{\left(\frac{N}{2}\right)^2+n_i^2}, \tag{19b}$$

$$p = -\frac{N}{2}+\sqrt{\left(\frac{N}{2}\right)^2+n_i^2}, \tag{19c}$$

where V is the applied voltage and χ is the electron affinity of semiconductor.

In our simulation, the piezoelectric charges are assumed to be distributed uniformly at the two ends of the n-type piezoelectric semiconductor within a width of W_{piezo} as shown in Figure 2(a). The length of the p-type GaN is 20 nm and the length of the n-type ZnO is 80 nm. The radius of the device is 10 nm. The n-type background doping concentration N_{Dn} is 1×10^{15} cm^{-3}. The maximum acceptor doping concentration $N_{\text{Ap max}}$ is 1×10^{17} cm^{-3} and the maximum donor doping concentration $N_{\text{Dn max}}$ is 1×10^{17} cm^{-3}. The doping fall-off constant ch is set to 4.66 nm. The temperature T is 300 K. More parameters of GaN and ZnO required in the simulation are displayed in Table 1.

The current density curves at various voltages under different strains are shown in Figure 2(b). Under negative (compressive) strains, the positive piezoelectric charges are created at the interface of the heterojunction and attract electrons to accumulate near the interface, which results in an increase of the built-in potential and a reduction of the saturation current density. On the contrary, under positive strain case, the negative piezoelectric charges are created at the interface of the heterojunction and attract the holes to accumulate near the interface, which leads to a reduction in the built-in potential and an increase of the saturation current density.

Figure 3(a) shows the distribution of electron concentrations at a fixed forward bias voltage of 2 V across the heterojunction under applied strain from –0.08% to 0.08%, displaying the redistribution of electrons. Under compressive strain, the electron concentration shows a peak at the interface of the junction where the positive piezoelectric charges are created. Inversely under tensile strain, the electron concentration shows a valley at the interface for the negative piezoelectric charges repel the electrons.

Figure 3(b) displays the distribution of hole concentrations at a fixed forward bias voltage of 2 V across the heterojunction under applied strain from –0.08% to 0.08%, showing the effect of the piezoelectric charges on the hole distribution. Under tensile strain, the hole concentration shows a peak at the interface of the heterojunction where

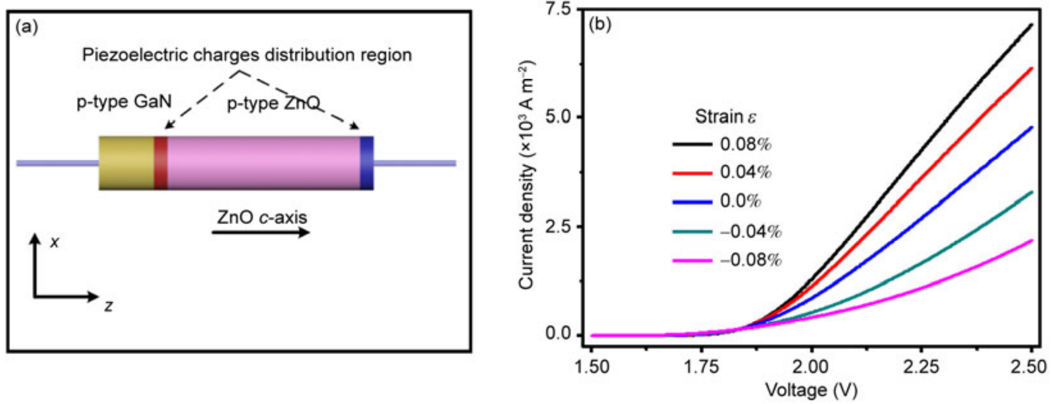

Figure 2 (a) Sketch of a piezoelectric heterojunction; (b) calculated current densities curves.

Table 1 Properties of p-type GaN and n-type ZnO at T=300 K

	χ(eV)	E_g(eV)	$\varepsilon_\perp, \varepsilon_{//}$	n_i (cm^{-3})	μ_n, μ_p (cm^2 (VS)$^{-1}$)	τ_n, τ_p (μs)
p-GaN	4.1	3.4	9.7	1.9×10^{-10}	900, 350	0.01, 0.01
n-ZnO	4.5	3.37	7.77, 8.91	1×10^{6}	200, 180	0.1, 0.1

the negative piezoelectric charges are created. While the device is under compressive strain, positive piezo-charges are created on the interface of the heterojuncion and repel the holes, therefore there is no peak at the vicinity of the heterojunction.

Moreover, we investigated the DC characteristics and carrier concentration distribution at various doping concentrations. The strain is fixed at 0.08% and the n-type background doping concentration N_{Dn} is set to $1\times10^{15}\ \mathrm{cm}^{-3}$. In the condition of $N_{\mathrm{Dn\ max}}=N_{\mathrm{Ap\ max}}$, the current density curves are plotted in Figure 4(a) corresponding to increasing $N_{\mathrm{Dn\ max}}$ from $1\times10^{16}\ \mathrm{cm}^{-3}$ to $9\times10^{16}\ \mathrm{cm}^{-3}$, which implies that the threshold voltage increases while $N_{\mathrm{Dn\ max}}$ decreases. We also investigate the current density at different background doping concentrations N_{Dn} by setting $N_{\mathrm{Dn\ max}}=N_{\mathrm{Ap\ max}}=1\times10^{17}\ \mathrm{cm}^{-3}$ and increasing N_{Dn} from $1\times10^{13}\ \mathrm{cm}^{-3}$ to $5\times10^{15}\ \mathrm{cm}^{-3}$, which shows little differences as shown in Figure 4(b). The numerical results suggest that the current-voltage characteristics depend on the donor and acceptor doping concentration distribution in our model. Figure 5(a) and (b) illustrate the distribution of electron and hole concentration at a fixed forward bias voltage of 2 V under a tensile strain of 0.08%.

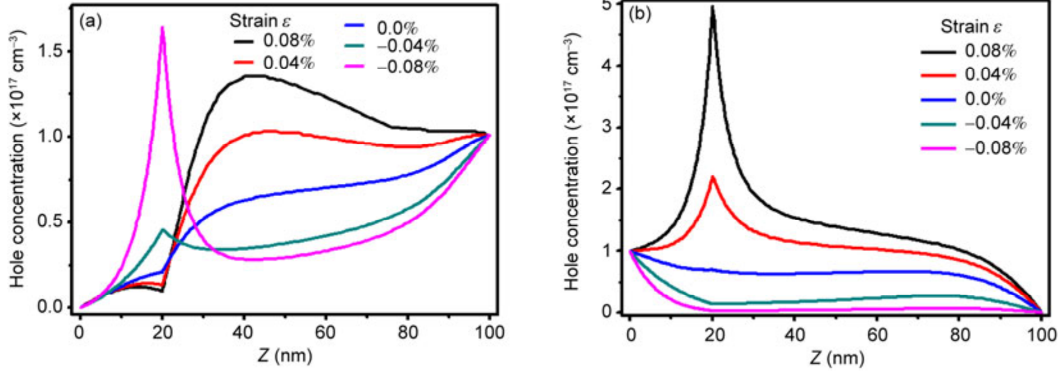

Figure 3 Distribution of electrons (a) and holes (b) at a fixed voltage of 2 V under various strain from −0.08 to 0.08%.

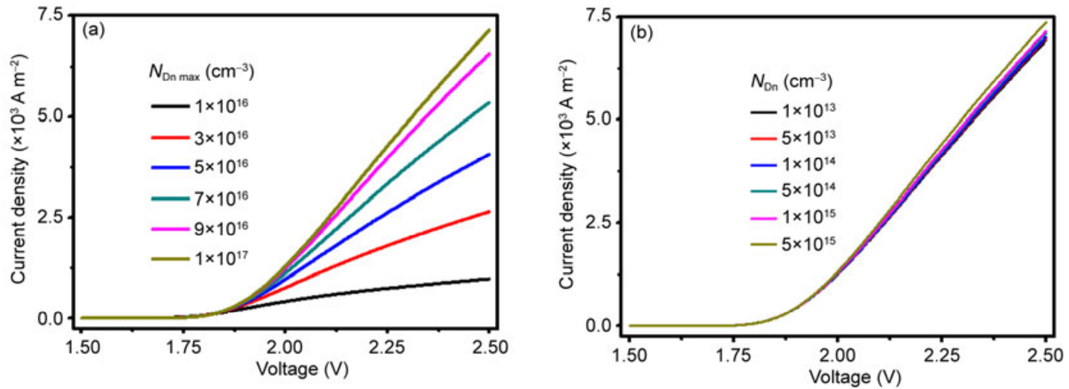

Figure 4 Calculated current densities at various maximum doping concentrations (a) and various n-type background doping concentrations (b).

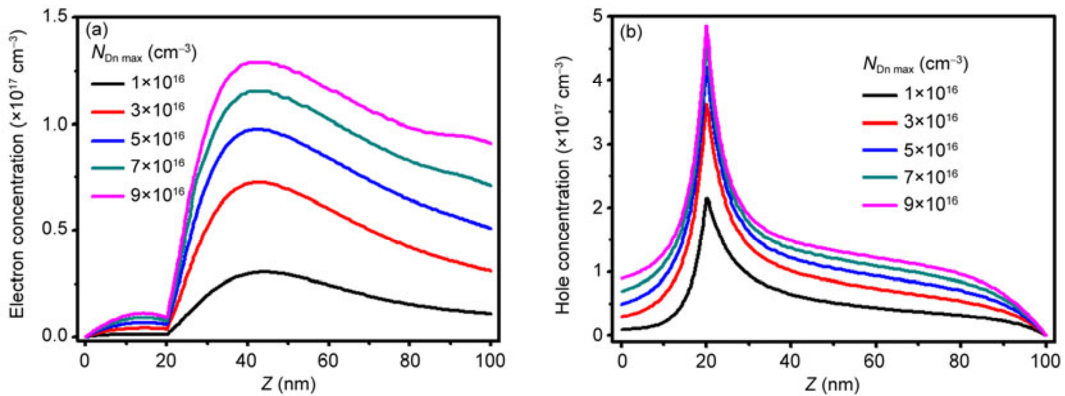

Figure 5 Distribution of electrons (a) and holes (b) at fixed voltage of 2 V at a fixed strain.

5 Conclusion

In summary, a model for an abrupt anisotype piezoelectric heterojunction is proposed to analyze the effect of the piezoelectric charges on the carrier transport behavior. This model uses a material configuration of p-n GaN-ZnO, which is used extensively in experimental design. The analytical solutions reveal the theoretical mechanism of piezoelectric heterojunctions. Numerical simulation is presented to depict the carrier transport process providing predictions of the piezoelectric heterojunction performance. Therefore, the theory presented here can be a guidance for the future experimental design of piezoelectric heterojunctions.

This work was partly supported by the Beijing Institute of Nanoenergy and Nanosystems, Chinese Academy of Sciences and the Fundamental Research Funds for the Central Universities (Grant No. Lzujbky-2013-35).

1 Wang Z L, Song J. Piezoelectric nanogenerators based on zinc oxide nanowire arrays. Science, 2006, 312: 242–246
2 Lin Y F, Song J H, Ding Y, et al. Piezoelectric nanogenerator using CdS nanowires. Appl Phys Lett, 2008, 92(2): 022105
3 Lu M Y, Song J, Lu M P, et al. ZnO-ZnS heterojunction and ZnS nanowire arrays for electricity generation. Acs Nano, 2009, 3(2): 357–362
4 Lin L, Lai C H, Hu Y, et al. High output nanogenerator based on assembly of GaN nanowires. Nanotechnology, 2011, 22(47): 475401
5 Hu Y F, Zhang Y, Lin L, et al. Piezo-phototronic effect on electroluminescence properties of p-Type GaN thin films. Nano Lett, 2012, 12(7): 3851–3856
6 Chen C Y, Zhu G, Hu Y, et al. Gallium nitride nanowire based nanogenerators and light-emitting diodes. Acs Nano, 2012, 6(6): 5687–5692
7 Wang X D, Song J H, Liu J, et al. Direct-current nanogenerator driven by ultrasonic waves. Science, 2007, 316(5821): 102–105
8 Qin Y, Wang X D, Wang Z L. Microfibre-nanowire hybrid structure for energy scavenging. Nature, 2008, 451(7180): 809–U5
9 Lee M, Bae J, Lee J, et al. Self-powered environmental sensor system driven by nanogenerators. Energ Environ Sci, 2011, 4(9): 3359–3363
10 He J H, Hsin C L, Liu J, et al. Piezoelectric gated diode of a single ZnO nanowire. Adv Mater, 2007, 19(6): 781–784
11 Han W H, Zhou Y H, Zhang Y, et al. Strain-gated piezotronic transistors based on vertical zinc oxide nanowires. Acs Nano, 2012, 6(5): 3760–3766
12 Liu Y, Yang Q, Zhang Y, et al. Nanowire piezo-phototronic photodetector: Theory and experimental design. Adv Mater, 2012, 24(11): 1410–1417
13 Gao Y, Wang Z L. Electrostatic potential in a bent piezoelectric nanowire. The fundamental theory of nanogenerator and nanopiezotronics. Nano Lett, 2007, 7(8): 2499–2505
14 Wang Z L. The new field of nanopiezotronics. Mater Today, 2007, 10(5): 20–28
15 Wang Z L. Nanopiezotronics. Adv Mater, 2007, 19(6): 889–892
16 Zhou J, Fei P, Gu Y D, et al. Piezoelectric-Potential-Control led Polarity-Reversible Schottky Diodes and Switches of ZnO Wires. Nano Lett, 2008, 8(11): 3973–3977
17 Wang Z L. Splendid one-dimensional nanostructures of zinc oxide: A new nanomaterial family for nanotechnology. Acs Nano, 2008, 2(10): 1987–1992
18 Wang Z L. ZnO nanowire and nanobelt platform for nanotechnology. Mat Sci Eng R, 2009, 64(3-4): 33–71
19 Wang Z L. Ten years' venturing in ZnO nanostructures: From discovery to scientific understanding and to technology applications. Chinese Sci Bull, 2009, 54(22): 4021–4034
20 Wang Z L. From nanogenerators to piezotronics-A decade-long study of ZnO nanostructures. Mrs Bull, 2012, 37(9): 814–827
21 Zhang Y, Liu Y, Wang Z L. Fundamental theory of piezotronics. Adv Mater, 2011, 23(27): 3004–3013
22 Zhang Y, Wang Z L. Theory of piezo-phototronics for light-emitting diodes. Adv Mater, 2012, 24(34): 4712–4718
23 Crowell C R, Sze S M. Current transport in metal-semiconductor barriers. Solid-state electronics, 1966, 9: 1035–1048
24 Sze S M. Physics of Semiconductor Devices. ed. 2nd. 1981, New York: Wiley
25 Schottky W. Halbleitertheorie der Sperrschicht. Naturwissenschaften, 1938, 26(52): 843–843
26 Bethe H A. MIT Radiat Lab Rep, 1942. 43: 12
27 Ikeda T. Fundamentals of Piezoelectricity. Oxford, UK: Oxford University Press, 1996
28 Maugin G A. Continuum Mechanics of Electromagnetic Solids. North-Holland: Amsterdam, 1988
29 Calow J T, Deasley P J, Owen J T, et al. A review of semiconductor heterojunctions. J Mater Sci, 1967, 2(1): 88–96
30 Palankovski V, Quay R. Analysis and Simulation of Hererostructure Devices. Wien, New York: Springer, 2004